energies

MDPI

Article

Performance of Common Rail Direct Injection (CRDi) Engine Using Ceiba Pentandra Biodiesel and Hydrogen Fuel Combination

T. M. Yunus Khan [1,2,*], Manzoore Elahi M. Soudagar [3,*], S. V. Khandal [4], Syed Javed [2], Imran Mokashi [5], Maughal Ahmed Ali Baig [6], Khadiga Ahmed Ismail [7] and Ashraf Elfasakhany [8]

1 Research Center for Advanced Materials Science (RCAMS), King Khalid University, P.O. Box 9004, Abha 61413, Saudi Arabia
2 Department of Mechanical Engineering, College of Engineering, King Khalid University, Abha 61421, Saudi Arabia; syedjavedme@gmail.com
3 Department of Mechanical Engineering, School of Technology, Glocal University, Delhi-Yamunotri Marg, SH-57, Mirzapur Pole, Saharanpur 247121, Uttar Pradesh, India
4 Department of Mechanical Engineering, Sanjay Ghodawat University, Kolhapur 416118, Maharashtra, India; sanjeevvkhandal@gmail.com
5 Department of Mechanical Engineering, Bearys Institute of Technology, Mangalore 574153, Karnataka, India; mokashi782@gmail.com
6 Department of Mechanical Engineering, CMR Technical Campus, Hyderabad 501401, Telangana, India; mabaig09@gmail.com
7 Department of Clinical Laboratory Sciences, College of Applied Medical Sciences, Taif University, P.O. Box 11099, Taif 21944, Saudi Arabia; khadigaah.aa@tu.edu.sa
8 Mechanical Engineering Department, College of Engineering, Taif University, P.O. Box 11099, Taif 21944, Saudi Arabia; ashr12000@yahoo.com or a.taha@tu.edu.sa
* Correspondence: yunus.tatagar@gmail.com (T.M.Y.K.); me.soudagar@gmail.com (M.E.M.S.)

check for updates

Citation: Khan, T.M.Y.; Soudagar, M.E.M.; Khandal, S.V.; Javed, S.; Mokashi, I.; Baig, M.A.A.; Ismail, K.A.; Elfasakhany, A. Performance of Common Rail Direct Injection (CRDi) Engine Using Ceiba Pentandra Biodiesel and Hydrogen Fuel Combination. *Energies* **2021**, *14*, 7142. https://doi.org/10.3390/en14217142

Academic Editor: Jeffrey S. Cross

Received: 18 August 2021
Accepted: 14 October 2021
Published: 1 November 2021

Abstract: An existing diesel engine was fitted with a common rail direct injection (CRDi) facility to inject fuel at higher pressure in CRDi mode. In the current work, rotating blades were incorporated in the piston cavity to enhance turbulence. Pilot fuels used are diesel and biodiesel of Ceiba pentandra oil (BCPO) with hydrogen supply during the suction stroke. Performance evaluation and emission tests for CRDi mode were carried out under different loading conditions. In the first part of the work, maximum possible hydrogen substitution without knocking was reported at an injection timing of 15° before top dead center (bTDC). In the second part of the work, fuel injection pressure (IP) was varied with maximum hydrogen fuel substitution. Then, in the third part of the work, exhaust gas recirculation (EGR), was varied to study the nitrogen oxides (NOx) generated. At 900 bar, HC emissions in the CRDi engine were reduced by 18.5% and CO emissions were reduced by 17% relative to the CI mode. NOx emissions from the CRDi engine were decreased by 28% relative to the CI engine mode. At 20%, EGR lowered the BTE by 14.2% and reduced hydrocarbons, nitrogen oxide and carbon monoxide by 6.3%, 30.5% and 9%, respectively, compared to the CI mode of operation.

Keywords: hydrogen (H_2); biodiesel of ceiba pentandra oil (BCPO); hydrogen fuel flow rate (HFR); exhaust gas recirculation (EGR); common rail direct injection (CRDi)

1. Introduction

Concerns about fossil fuels depletion and economic viability along with environmental regulations have projected biodiesels as a feasible option that works for the internal combustion (IC) engine. There has been a surge in the implementation of diesel engines in the automotive sector which are energy efficient, durable and reliable. Despite these credits, the NOx emissions are of critical concern. Dual fuel utilization has resulted in improved performance of diesel engines with considerable NOx reduction [1–3]. The hydrogen-diesel engine (heavy duty) was reported to have smooth operational condition at 98% H_2 composition at lower loads. A similar operational capacity was noticed at 85%

H_2 composition with medium load. NOx emissions were lowered by 75% with the recirculation of exhaust gas in the hydrogen-diesel dual fuel (DF) operation [4]. The hydrogen supply was varied from 0 to 55%; the NOx emissions were reduced with an increase in H_2 supply contrary to the higher compression ratio (CR) [5]. Diesel engine operation using natural gas and eucalyptus methyl ester at different rates of hydrogen, running at 1500 rpm, showed peculiar results. At varied quantities of natural gas, 25% H_2 and a constant amount of eucalyptus biodiesel reduced the brake specific fuel consumption (BSFC) by 10%. The increased supply of NG and H_2 accelerated the rate of heat release and elevated the peak pressure (PP). A shorter ignition delay (ID) compensated for the rise in heat release rate (HRR) and peak pressure (PP) [6].

Pilot fuels such as hydrogen, producer gas, or a blend of both were used in the diesel engine. The peak pressure was recorded for 30% use of hydrogen, but further increase in the quantity showed pressure reduction for different loads. Another investigation revealed PP increase for 13% to 40% load and with load about 80% reduced the PP. Reduction in the rate of heat release was found with the use of fuel blend comparatively to the use of diesel [7]. The parametric study was conducted considering factors such as speed of engine, ratio of equivalence, % of hydrogen content, timing of fuel injection and recirculation of exhaust gas (EGR). The information obtained from this parametric study is used in model making. Validation of NOx model can form a basis for research [8]. The inclusion of hydrogen caused increase in the NOx emissions. The conversion of nitrogen oxide to nitrogen dioxide was initiated post combustion in a DF engine [9]. Hydrogen utilization in diesel engine significantly reduced emissions such as carbon monoxide relative to use of fossil fuels [10]. Hydrogen addition to biogas at higher loads affected the combustion thereby enhancing the HRR and PP. A 5% H_2 usage at all loads had no significant change on the performance and emission features, but an H_2 supply surpassing 5% yielded less emissions and better performance [11]. The use of hydrogen gas facilitates functioning of the engine at a higher ratio of compression [12]. The outcomes of using hydrogen gas as fuel in a diesel engine were as follows: Enhancement in the BTE was collateral with emission reduction, but NOx content was unchanged [13,14]. Timing of ignition was 27° before TDC, and 15% EGR improved the BTE of DF engine and lowered the emissions at varied hydrogen supply rates [15]. The CRDi engine operated at an internal gas pressure of 900 bar and 10° bTDC fuel injection timing was found to provide improved BTE. It was also reported that the implementation of EGR from exhaust minimized the NOx emission [16]. Studies related to CRDi engine performance were conducted for variables such as fuels, and other governing parameters showed improved engine work with low emissions [17–20].

From the extensive literature review, it could be concluded that scarce literature is available on performance testing of CRDi engines with influencing parameters, namely, rate of hydrogen supply, fuel injection pressure and recirculation of exhaust gas with hydrogen and BCPO as fuels. Thus, the research undertaken provided evaluation data for a parametric study using diesel-hydrogen and BCPO-hydrogen as fuels in a CRDi engine incorporating combustion chamber modifications.

2. Test Procedure Details

2.1. Combustion Fuels Used

Hydrogen and air are supplied in suction stroke along with injection of pilot fuel diesel/BCPO. Table 1 is a representation of fuel properties obtained using ASTM standards. Hydrogen properties are depicted in Table 2.

Table 1. Diesel and BCPO characteristic features.

Properties	Diesel Fuel	BCPO Fuel
Chemical composition	$C_{12}H_{23}$	$C_9H_{18}O_2$
Kinematic viscosity at 40 °C (cSt)	2.5	5.1
Calorific Fuel Value (kJ/kg)	44,000	38,900
Density at 15 °C (kg/m^3)	832	890
Cloud Temperature Point (°C)	−2	4
Pour Temperature Point (°C)	−5	5.5
Flash Temperature Point (°C)	66	205

Table 2. Properties of H_2 [12] (adapted with permission from International Journal of Hydrogen Energy, Elsevier B.V., License Number: 5170760634154).

Properties	Hydrogen Fuel
Chemical composition	H_2
Temperature of auto ignition (K)	858
Minimum energy for ignition (mJ)	0.02
Flammable range (% volume in air)	4–75
Mass basis Stoichiometric air fuel ratio	34.3
Density at 1 bar and 15 °C	0.0838
Net value of heating (MJ/kg)	119.93
Velocity of flame (cm/s)	265–325
Octane grade number	130

2.2. Test Set-Up

Existing single cylinder diesel engine was fitted with CRDi facility, and tests were conducted in CRDi mode at higher pressure. Engine specifications are specified in Table 3. Figure 1 shows the layout of a computerized CRDI diesel test engine, which shows the mounting of necessary instruments onto the engine. A piezoelectric pressure reading device is utilized to measure in-cylinder gas pressure. Measurements of combustion parameters and performance factors were obtained at different loads. HFR was controlled within the range 0.11–0.24 kg/h at 17.5 CR. A digital flow meter was used to measure HFR. A wet type flame arrester was employed to avoid backfiring during the tests. Tests were conducted thrice to record the performance resulting from each fuel combination. The average of the recorded readings was depicted as reliant-accurate data. An exhaust gas analyzer (EGA) and smoke meter were used to get the emissions.

Table 3. Specifications of CRDi Diesel engine.

Parameters	Specifications
Type of Engine	Cylinder: 1 Stroke: 4
Injection pressure	600–1000 bar
Cooling system	Water cooling
Type of fuel used	Diesel/Biodiesel
Rated power	5.2 kW at 1500 RPM
Torque at full load	0.033 kg-m
Cubic capacity	0.661 L
Bore diameter	0.0875 m
Stroke Length	0.11 m
Ratio of Compression (RC)	17.5:1

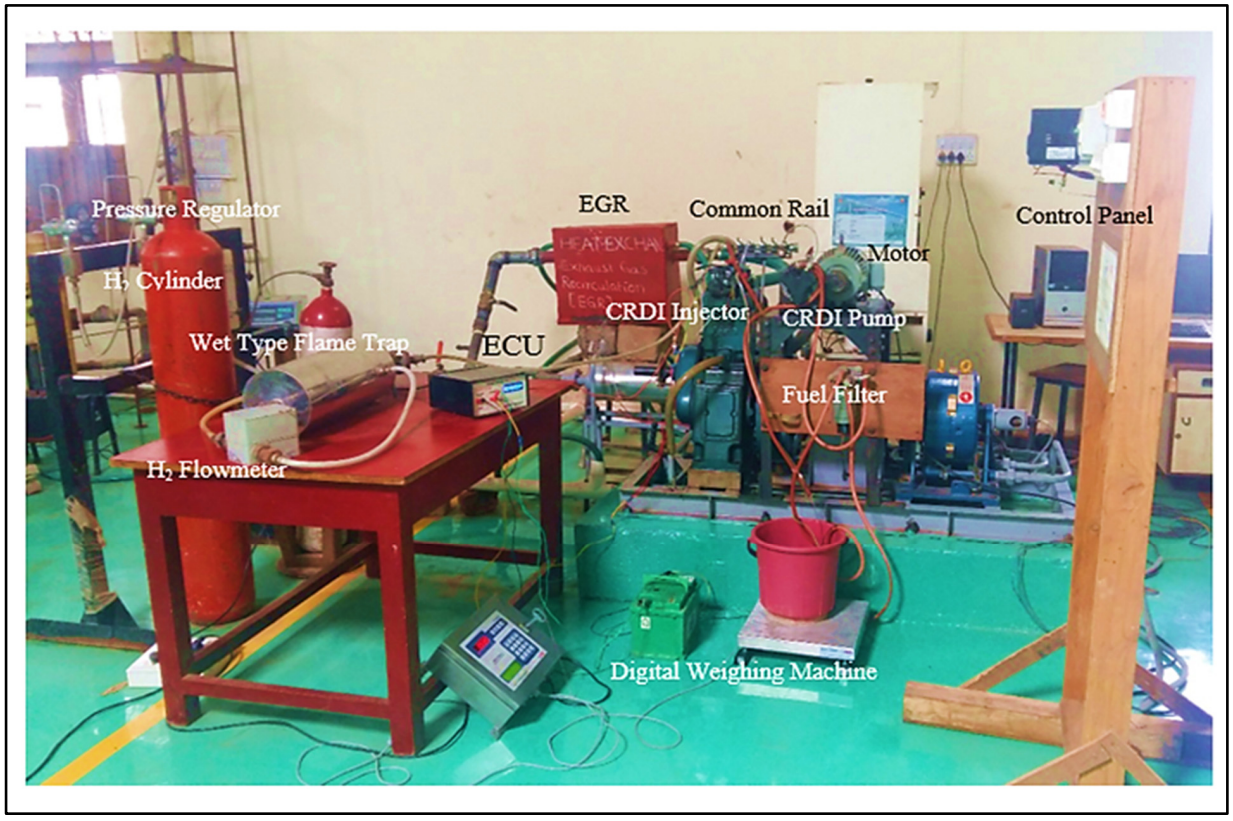

Figure 1. Layout of computerized CRDI diesel test engine.

Equation (1) provides the rate of heat released at every CA. The calculation was accounted for 100 cycles.

$$Q = \left(\frac{\gamma}{\gamma - 1}\right) p.\,dv + \left(\frac{1}{\gamma - 1}\right) v.\,dp + Q_{wall} \quad (1)$$

The assumption of ideal combustible gas was considered. The gas specific heat is dependent on temperature [21]. The Hohenberg equation was incorporated to calculate heat transfer through the cylinder wall [21]. The wall temperature was assumed to be 723 K [22].

2.3. Modifications in Piston

The rates of heat transfer and mixing of fuels with air are several times better in turbulent flows which is very much essential for the efficient performance of an IC engine. To infuse this advantage the piston is modified by ancillary attachment of rotor blades fitted in the piston cavity. The CAD model of the altered piston design is presented in Figures 2 and 3. A regular standard piston and the rotor blade incorporated modified piston are shown in Figure 4a,b, respectively. This is provided in an earlier paper by the authors [23] (adapted with permission from Arabian Journal for Science and Engineering, Springer, License Number: 5163190256247).

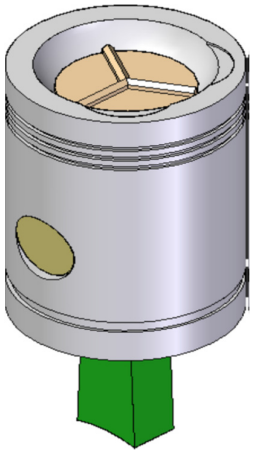

Figure 2. Modified piston [23].

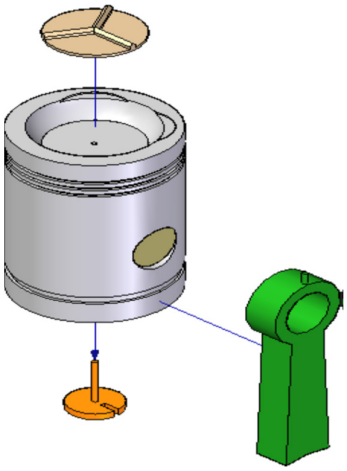

Figure 3. Exploded view of modified engine piston [23].

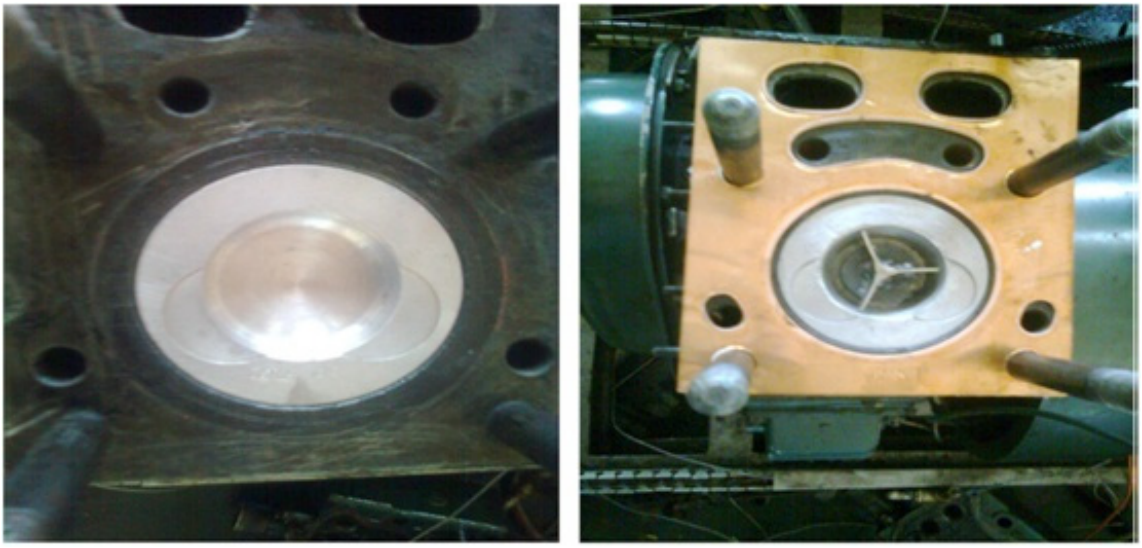

Figure 4. (**a**). Standard piston [23]. (**b**). Modified piston [23].

3. Test Data Analysis

Operating conditions in CI and CRDi mode has been provided in Table 4.

Table 4. Operating conditions in CI and CRDi mode.

Mode of Operation	Operating Conditions
CI	IT—23.5° bTDC, IOP—220 bar, CR—17.5, hemispherical combustion chamber, Fuel–Diesel, injector with 3 holes, 0.3 mm hole diameter CRDi
Case 1	IT—15° bTDC, IP—700 bar, CR—17.5, modified combustion chamber, Fuel–Diesel/BCPO with HFR variable, injector with 7 holes, 0.1 mm hole diameter
Case 2	IT—15° bTDC, IP—Variable, CR—17.5, modified combustion chamber, Fuel–Diesel/BCPO with HFR fixed, injector with 7 holes, 0.1 mm hole diameter
Case 3	IT—15° bTDC, IP—900 bar, CR—17.5, modified combustion chamber, Fuel–Diesel/BCPO with HFR fixed, EGR—variable, injector with 7-holes, 0.1 mm hole diameter

3.1. Influence of Flow Rate of Hydrogen

In this section, a CRDi engine working on DF has been examined for its performance at varied HFR. An IT of 10° bTDC and IP of 600 bar were set for CRDi working using diesel/BCPO fuel with modified piston. The operating conditions were set at IT of 23° bTDC and 205 bar IOP with combustion chamber of hemispherical shape in CI mode. The results for the CRDi engine were compared with CI mode.

3.1.1. Brake Thermal Efficiency

Brake thermal efficiency of diesel engine was calculated using Equation (2).

$$\eta_{th} = \frac{BP \times 3600}{[(m_f \times C_v)\, fuel + (m_g \times C_v)g]} \times 100 \quad (2)$$

where:

$(m_f\, xC_v)$ fuel—Mass of fuel x Calorific value of fuel;
$(m_g xC_v)g$—Mass of gas x Calorific value of gas;
BP—Brake power.

Brake power of an engine calculated with Equation (3).

$$BP = \frac{2\pi NT}{60x1000}\text{kW} \quad (3)$$

The BTE of the engine in response to HFR and load is shown in Figure 5. BTE rise could be seen from the plot. This increase in BTE can be attributed to proper combustion resulting from the temperature rise in the cylinder, which could be on account of the rapid hydrogen burning speed. At all loads, diesel fuel resulted in improved performance relative to BCPO. This could be due to lower specific fuel consumption and better combustion qualities of diesel as compared to BPCO. The BTE for BCPO operated CRDi engine in DF mode exhibited 13.6% reduction in comparison to diesel operated CRDi engine at 17.5 CR and 80% load with 0.22 kg/h HFR. HFR of more than 0.22 kg/h started knocking combustion. Hence the maximum possible HFR was 0.22 kg/h. Similar results could be seen in the literature [10,15].

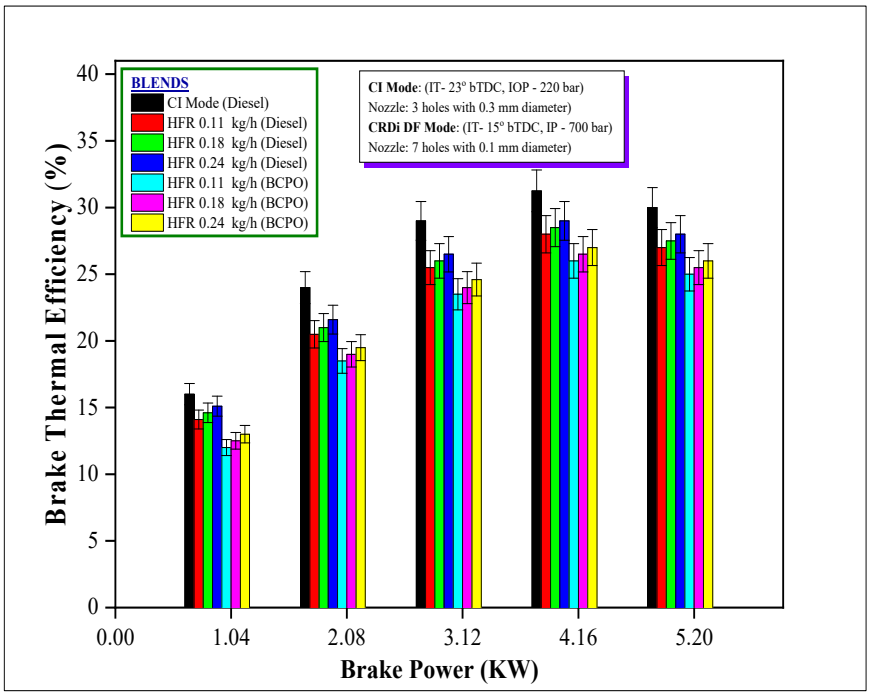

Figure 5. HFR and BP influence on CRDi engine BTE.

3.1.2. Emission Component Data

The variations in HFR and brake power affect the emissions of HC and CO which are represented in Figures 6 and 7, respectively. The plots reveal that hydrogen induction into the CRDi engine along with BCPO reduced the emissions at different loads. Low carbon content of the fuel mixture is attributed to this reduction of emission. Faster rate of combustion is also a probable factor for the obtained trend. At working conditions of 80% load, 17.5 CR and HFR 0.24 kg/h yielded similar HC emissions, contrary to which CI mode produced less CO. Similar results were reported in the literature [10,12].

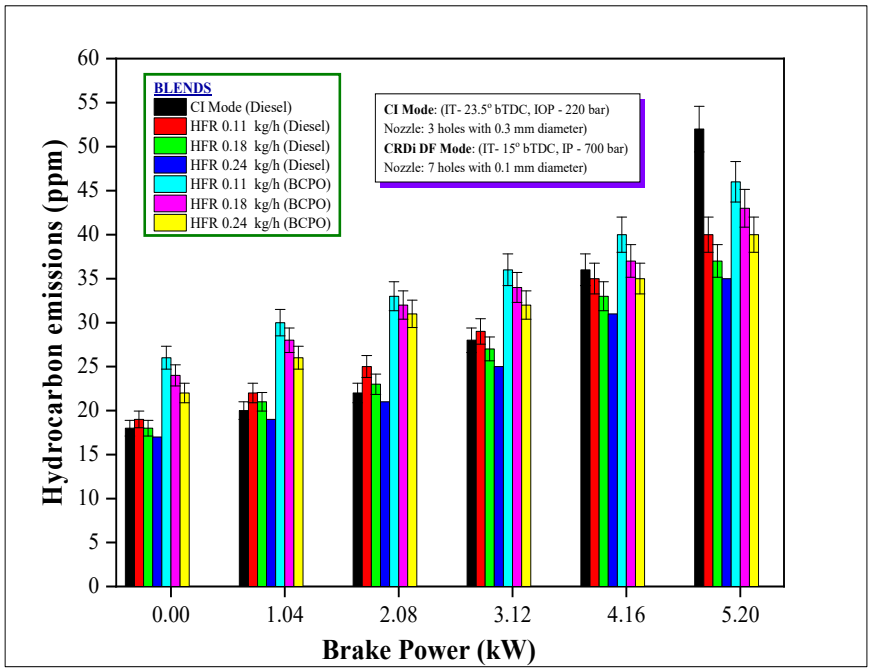

Figure 6. HFR and BP influence on CRDi engine HC emissions.

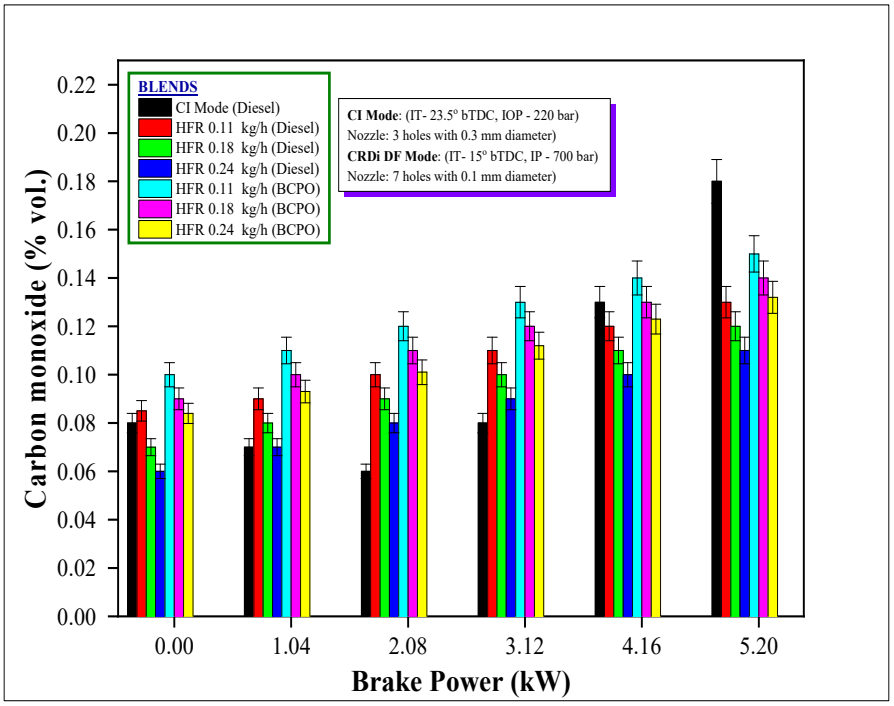

Figure 7. HFR and BP influence on CRDi engine CO emissions.

The HFR and BP influence on emissions of NOx in the CRDi engine is shown in Figure 8. At all loads, NOx emission increased at higher HFR. The likely reason could be lower ID and enhanced HRR resulting in raised temperature caused by the higher flame speed of hydrogen combustion. Use of BCPO resulted in NOx reduction because of ID increase and lower HRR. Under the conditions of 80% loading, 17.5 CR and 0.24 kg/h HFR, NOx reduction was better for the CRDi engine as compared to the CI mode of operation. Similar results were revealed in the literature [7,8].

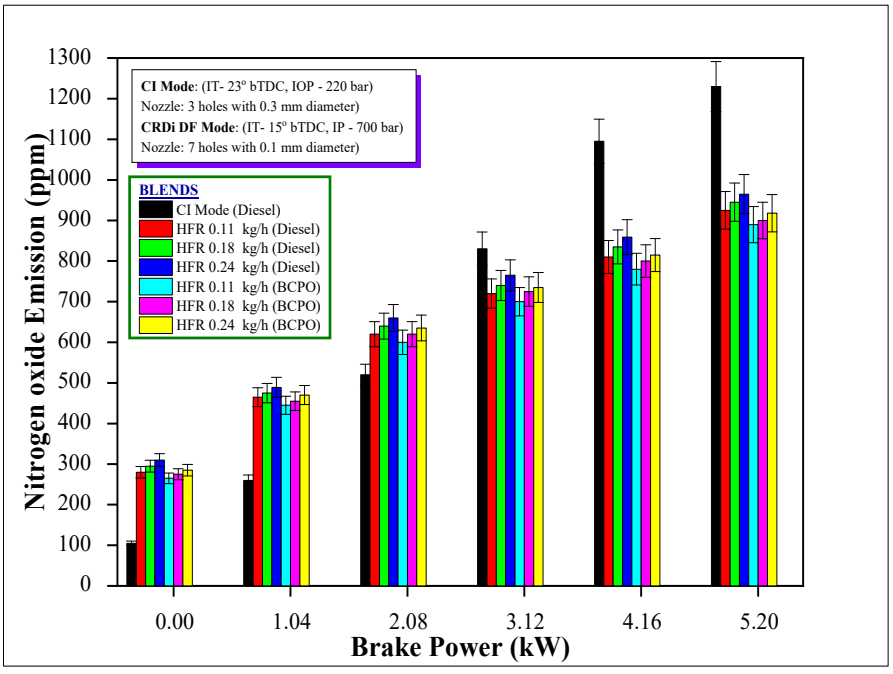

Figure 8. HFR and BP influence on CRDi engine NOx emission.

3.2. IP Variation Influence on CRDi Engine Performance

The performance of the CRDi engine caused by fuel IP variation from 600 bar to 1000 bar is described in this section. Engine test conditions selected for the study were IT of 15° bTDC and 0.24 kg/h constant HFR.

3.2.1. Brake Thermal Efficiency

Figure 9 is a graph showing the influence of fuel IP on CRDi engine BTE. For all loads, IP of 900 bar showed higher BTE as compared to other IP selected. The reason could be that better atomization facilitated an improved air–fuel mixing with the faster combustion of the mixture leading to a higher BTE. Further wall wetting could be the contributing factor for BTE decrement at maximum fuel IP. At the stated working conditions, CRDi engine with BCPO showed lower BTE and a marginal increase in BTE was noticed with diesel. The literature has highlighted similar observations [19,24,25].

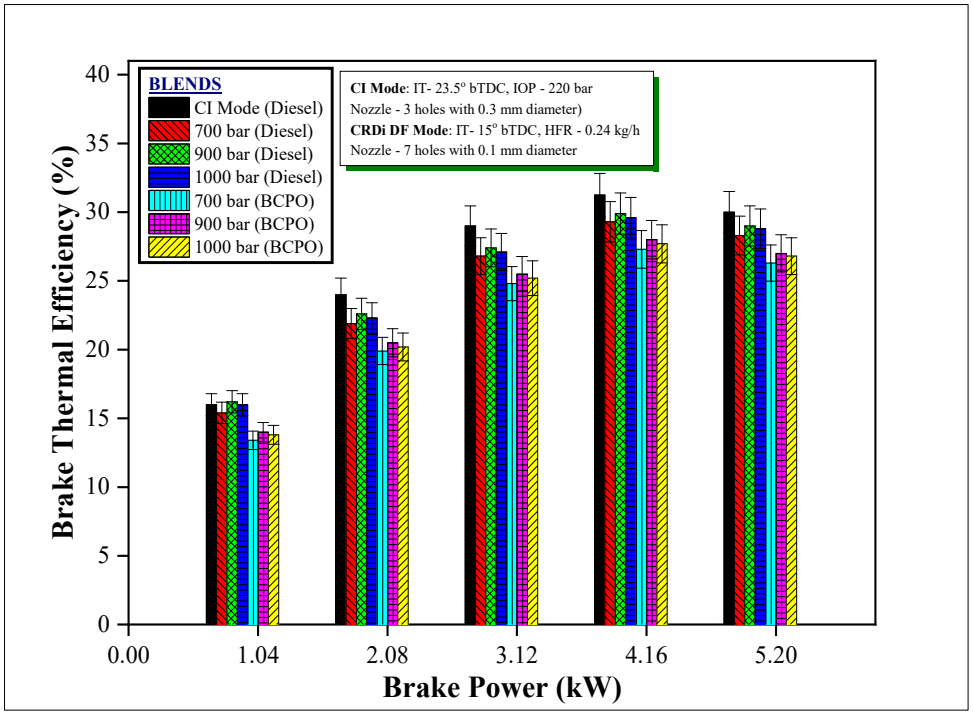

Figure 9. IP and BP influence on CRDi engine BTE.

3.2.2. Emission Component Data

Figures 10 and 11 are a representation of the HC and CO emissions with IP and BP, respectively. Increases in HC and CO emissions were observed with load. At a pressure of 900 bars, the emissions were less at all loads due to proper fuel mix and better combustion as compared to other IP selected. The flame speed of hydrogen being higher might have contributed to proper and faster combustion thereby lowering the emissions. Under working conditions of 80% load, 0.24 kg/h HFR and 900 bar IP with BCPO, the HC and CO emissions decreased relative to CI mode. Similar results were reported in the literature [18,25].

CRDi engine NOx emissions with variation in IP and BP are shown in Figure 12. NOx production could increase due to higher combustion temperature prevailing in the combustion chamber. Hydrogen's higher flame speed and higher HRR of CRDi engine led to increases in cylinder temperature and pressure which could be labeled as the cause for increase in NOx. Under the specified working conditions, reduced NOx emissions was recorded with EGR of 20% as compared to CI mode. Similar results were reported in the literature [4,8,9,15].

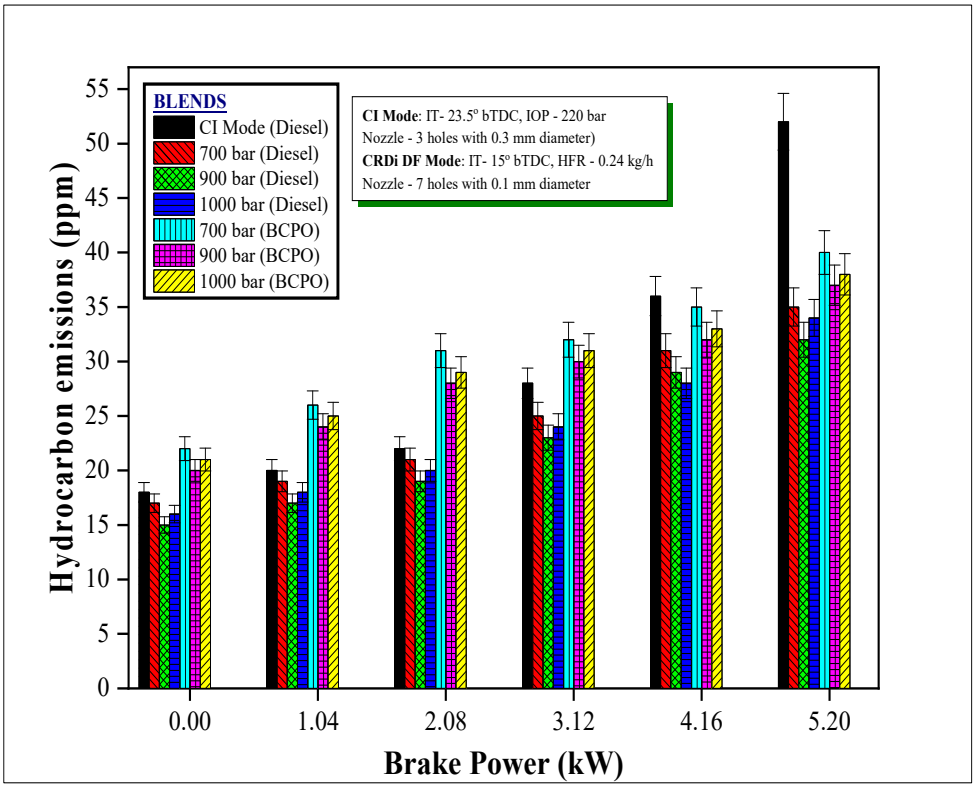

Figure 10. IP and BP influence on CRDi engine HC emissions.

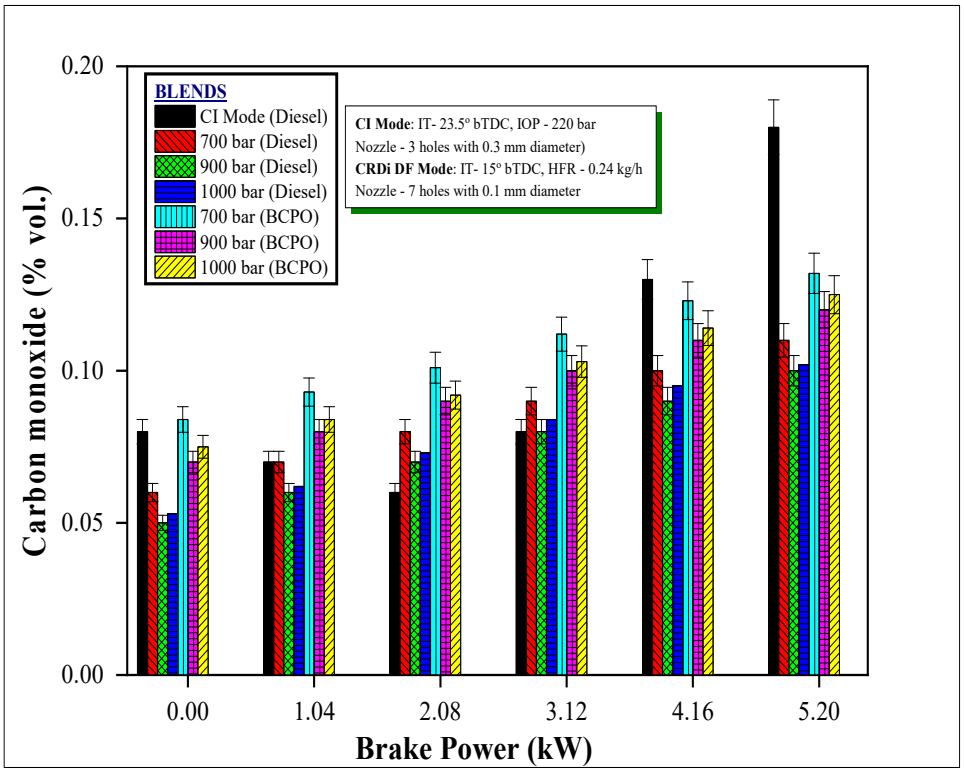

Figure 11. IP and BP influence on CRDi engine CO emissions.

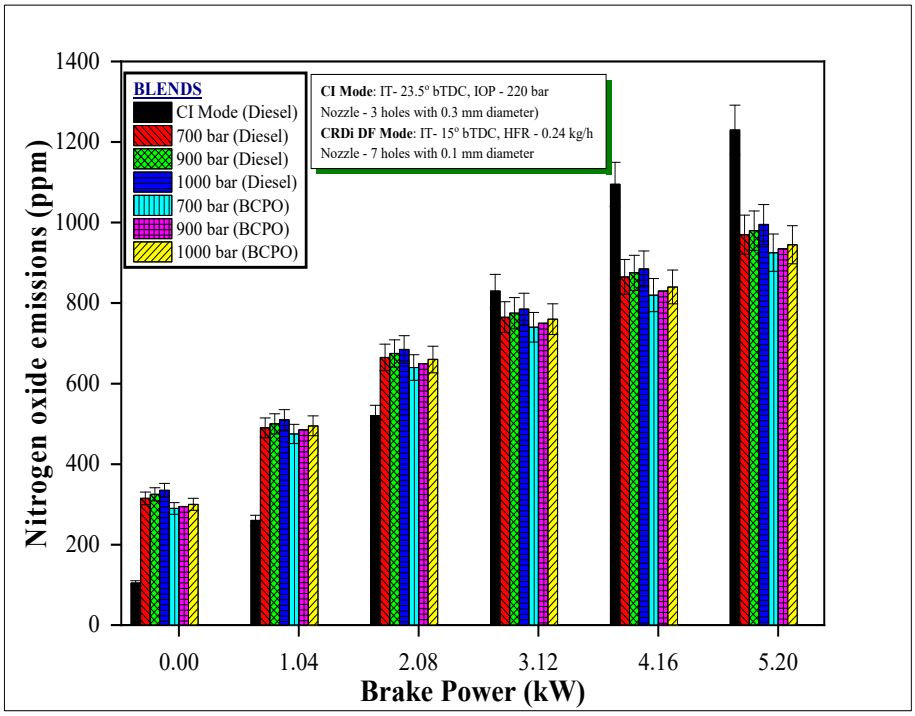

Figure 12. IP and BP influence on CRDi engine NOx emissions.

3.3. EGR Influence on CRDi Engine Performance

EGR at various percentages from 15 to 25% in a step of 5% was supplied to the CRDi engine to study the NOx emissions produced. This section presents the influence of EGR variation on the operating capability of the CRDi engine. Test conditions incorporated were IT of 15° bTDC, 0.24 kg/h HFR and 900 bar IP. EGR was estimated using the relation given in Equation (4).

$$EGR = \frac{[CO_2]\text{intake} - [CO_2]ambient}{[CO_2]\text{exhaust} - [CO_2]ambient} \quad (4)$$

3.3.1. Performance: Brake Thermal Efficiency

Figure 13 depicts EGR and BP influence on CRDi engine BTE. BTE decrement was noticed at all loads with EGR increment. The charge dilution could be a reason for the trend. It was seen that BTE decreased when the EGR rate increased, and this trend might be due to the predominant charge dilution effect of EGR with air inflow. EGR employed showed a negative effect on the BTE, chemical and thermal effects associated with EGR. The decreased BTE could also be because of the partial replacement of inhaling air by EGR which lowered the volumetric efficiency of the engine. The addition of burnt gas retarded the chemical kinetics due to the reduction in the active free radicals taking part in the pre-ignition chemical reactions. Under the 80% loading condition, specified HFR and IP BTE reduced. Similar results were reported in the literature [4,9,15].

3.3.2. Emission Component Data

Emissions of HC and CO in a CRDi engine under the influence of EGR are presented in Figures 14 and 15, respectively. The mixing of EGR with the inhaling air lowers the mixture strength in terms of reduction in oxygen concentration which decreased the combustion temperature. This could be the reason for increased tail pipe HC and CO levels in the exhaust gas. At higher EGR rates, the burning of injected fuel was suppressed due to more CO_2 in the mixture which lowers combustion temperature resulting in incomplete fuel burning. Large ID and reduced HRR witnessed an increment in the emissions of HC and CO at EGR of 25%. With BCPO, the emissions were lower for HC and CO emissions

relative to the use of diesel at specified working conditions at 15% EGR. Similar results were reported in the literature [4,8,9,15].

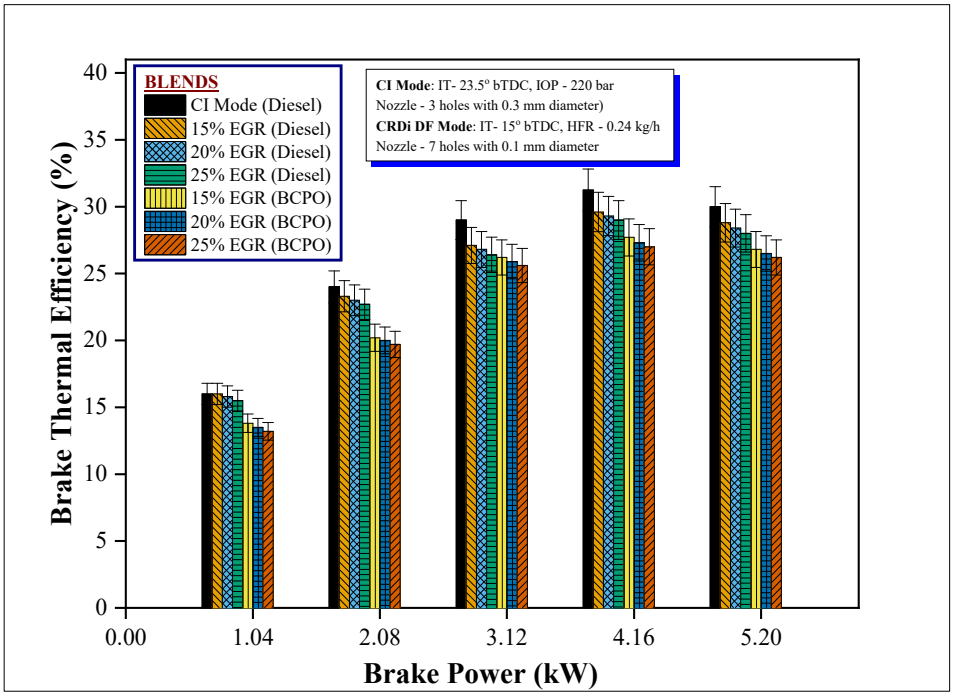

Figure 13. EGR and BP influence on CRDi engine BTE.

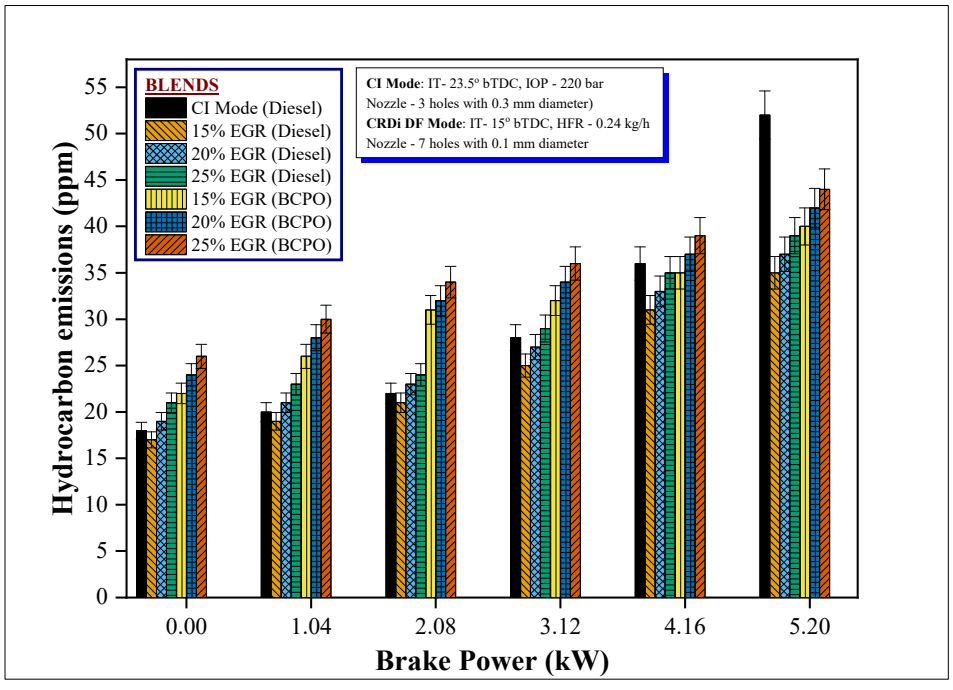

Figure 14. EGR and BP influence on CRDi engine HC emissions.

Figure 16 shows the EGR and BP influence on NOx emissions. NOx emissions recorded were higher at increased loads than at lesser loads. The rapid burning of hydrogen improved combustion which was due to lower ID and enhancing the temperature led to higher NOx emission. When EGR was inducted along with air, the concentration of oxygen in the mixture was reduced which decreased ID, retarding the HRR and the combustion

temperature. Hence a decrease in engine out NO_x in the exhaust was reported. The CRDi engine with high EGR rates of 25% yielded lower NO_x compared to the lesser EGR rates of 15% and 20%. Better combustion prevailed at 900 bar IP due to better air fuel mix. NOx emissions were low at 25% EGR but BTE reduction was also noticed. A 20% EGR can be calculated as an appropriate selection with a slight sacrifice in BTE. At 20% EGR and specified working conditions, the use of BCPO lowered the NOx emissions relative to CI mode. Slightly high NOx emissions were recorded with hydrogen-diesel use. Hydrogen-BCPO exhibited better combustion and thus reduced NOx emissions. Similar results were reported in the literature [4,8,9,15].

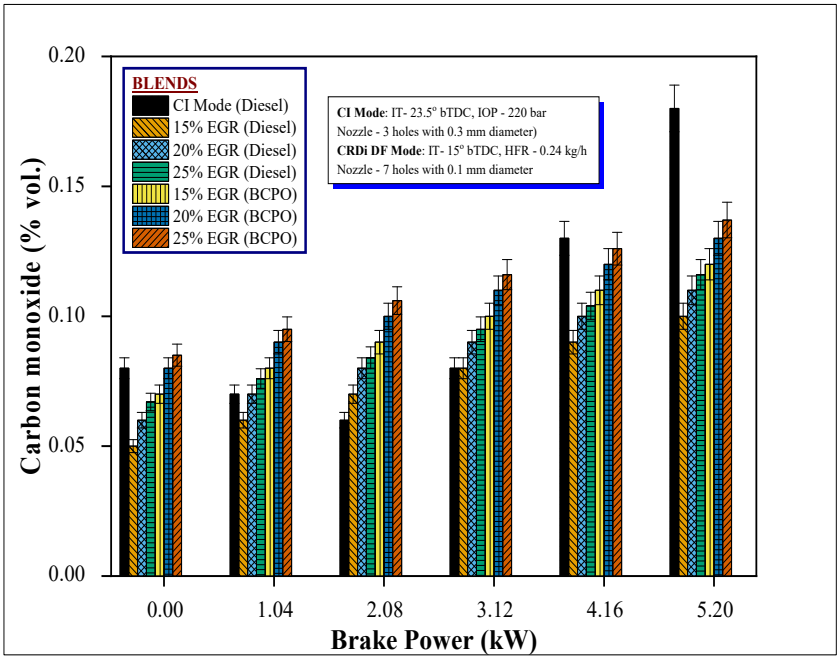

Figure 15. EGR and BP influence on CRDi engine CO emissions.

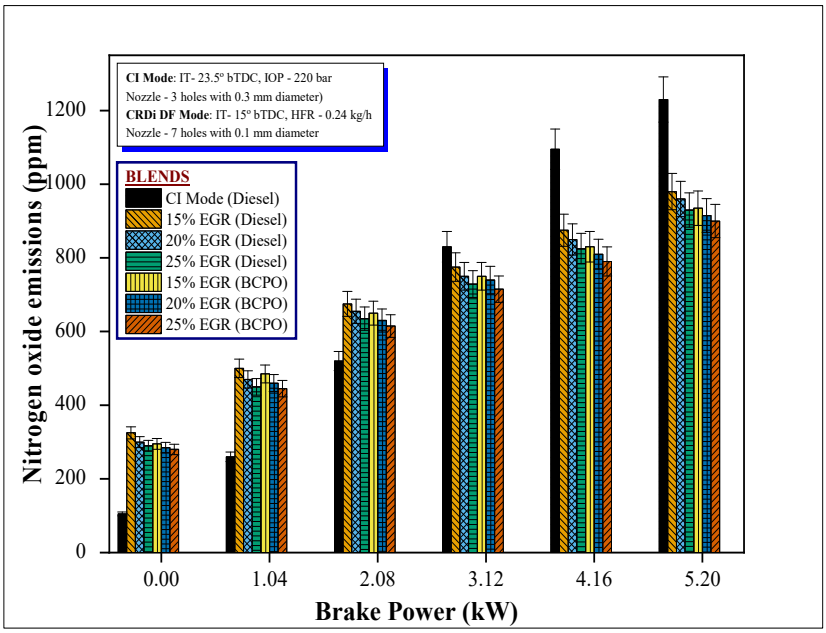

Figure 16. EGR and BP influence on CRDi engine NOx emissions.

4. Conclusions

A comprehensive presentation was carried out of a CRDi engine performance using dual fuel, namely, diesel/BCPO and hydrogen at various control parameters such as HFR, EGR and IP. The data obtained by experimentation yields the following conclusions:

- Hydrogen infusion reduced the pilot fuel content. At operating parameters of 0.24 kg/h HFR, 900 bar IP with combustion chamber modifications collaborated to give CRDi engine a better performance with lower emissions.
- At 0.24 kg/h HFR, the CRDi engine provided 7.8% reduced BTE and redesigned combustion chamber relative to diesel-operated CI mode.
- At optimum operating conditions, HC emissions in CRDi engine were reduced by 18.5%, and CO emissions were decreased by 17% relative to the CI mode. NOx emissions in CRDi engine were decreased by 28% relative to the CI mode.
- At 20% EGR lowered the BTE by 14.2% and reduced hydrocarbons, nitrogen oxide and carbon monoxide by 6.3%, 30.5% and 9%, respectively, compared to the CI mode of operation.

The aim of the article was to show that a significant operating capability was observed in a CRDi engine utilizing diesel/BCPO and hydrogen fuel combination and combustion chamber modification. The induction of these dual fuels caters to national energy conservation by limiting fossil fuel use.

Author Contributions: Conceptualization, S.V.K. and T.M.Y.K.; methodology, S.V.K. and M.E.M.S.; validation, S.J. and M.E.M.S.; formal analysis. T.M.Y.K.; investigation, S.V.K.; resources, S.J. and M.A.A.B.; writing—original draft preparation, S.V.K. and I.M.; writing—review and editing, T.M.Y.K. and M.E.M.S.; project administration, S.J; funding acquisition, S.J. and M.A.A.B.; research support, K.A.I.; writing review and funding acquisition, A.E. All authors have read and agreed to the published version of the manuscript.

Funding: This work was funded by at King Khalid University under grant number R.G.P 2/107/41 and Taif University Researchers Supporting Project Number TURSP-2020/117, Taif University, Taif, Saudi Arabia.

Institutional Review Board Statement: Not applicable.

Informed Consent Statement: Not applicable.

Data Availability Statement: Not applicable.

Acknowledgments: The author extend his appreciation to the Deanship of Scientific Research at King Khalid University for funding this work through research groups program under grant number R.G.P 2/107/41. This study was supported by Taif University Researchers Supporting Project Number TURSP-2020/117, Taif University, Taif, Saudi Arabia.

Conflicts of Interest: The authors declare no conflict of interest.

Nomenclature

CRDi	Common rail direct injection
DF	Dual fuel
H_2	Hydrogen
CI	Compression ignition
IC	Internal combustion
ID	Ignition delay
IOP	Injector opening pressure
IP	Injection pressure
IT	Injection timing
EGR	Exhaust gas recirculation
CA	Crank angle
CR	Compression ratior

bTDC	Before top dead centre
IT	Injection timing
BCPO	Biodiesel of ceiba pentandra oil
HFR	Hydrogen fuel flow rate
BSFC	Brake specific fuel consumption
HRR	Heat release rate
PP	Peak pressure
NOx	Oxides of nitrogen
HC	Hydrocarbon
CO	Carbon monoxide
NG	Natural gas

References

1. Abedin, M.J.; Imran, A.; Masjuki, H.H.; Kalam, M.A.; Shahir, S.A.; Varman, M.; Ruhul, A.M. An overview on comparative engine performance and emission characteristics of different techniques involved in diesel engine as dual-fuel engine oper-ation. *Renew. Sustain. Energy Rev.* **2016**, *60*, 306–316. [CrossRef]
2. Bora, B.J.; Saha, U.K. Experimental evaluation of a rice bran biodiesel—Biogas run dual fuel diesel engine at varying compression ratios. *Renew. Energy* **2016**, *87*, 782–790. [CrossRef]
3. Kumar, M.S.; Nataraj, G.; Selvan, S.A. A comprehensive assessment on the effect of high octane fuels induction on engine's combustion behaviour of a Mahua oil based dual fuel engine. *Fuel* **2017**, *199*, 176–184. [CrossRef]
4. Dimitriou, P.; Kumar, M.; Tsujimura, T.; Suzuki, Y. Combustion and emission characteristics of a hydrogen-diesel du-al-fuel engine. *Int. J. Hydrog. Energy* **2018**, *43*, 13605–13617. [CrossRef]
5. Sharma, P.; Dhar, A. Compression ratio influence on combustion and emissions characteristic of hydrogen diesel dual fuel CI engine: Numerical Study. *Fuel* **2018**, *222*, 852–858. [CrossRef]
6. Tarabet, L.; Lounici, M.; Loubar, K.; Khiari, K.; Bouguessa, R.; Tazerout, M. Hydrogen supplemented natural gas effect on a DI diesel engine operating under dual fuel mode with a biodiesel pilot fuel. *Int. J. Hydrog. Energy* **2018**, *43*, 5961–5971. [CrossRef]
7. Dhole, A.; Lata, D.; Yarasu, R. Effect of hydrogen and producer gas as secondary fuels on combustion parameters of a dual fuel diesel engine. *Appl. Therm. Eng.* **2016**, *108*, 764–773. [CrossRef]
8. Kumar, M.; Tsujimura, T.; Suzuki, Y. NOx model development and validation with diesel and hydrogen/diesel dual-fuel system on diesel engine. *Energy* **2018**, *145*, 496–506. [CrossRef]
9. Li, H.; Liu, S.; Liew, C.; Li, Y.; Wayne, S.; Clark, N. An investigation on the mechanism of the increased NO_2 emissions from H_2-diesel dual fuel engine. *Int. J. Hydrog. Energy* **2018**, *43*, 3837–3844. [CrossRef]
10. Tsujimura, T.; Suzuki, Y. The utilization of hydrogen in hydrogen/diesel dual fuel engine. *Int. J. Hydrog. Energy* **2017**, *42*, 14019–14029. [CrossRef]
11. Verma, S.; Das, L.; Kaushik, S.; Tyagi, S. An experimental investigation of exergetic performance and emission characteristics of hydrogen supplemented biogas-diesel dual fuel engine. *Int. J. Hydrog. Energy* **2018**, *43*, 2452–2468. [CrossRef]
12. Saravanan, N.; Nagarajan, G.; Dhanasekaran, C.; Kalaiselvan, K. Experimental investigation of hydrogen port fuel injection in DI diesel engine. *Int. J. Hydrog. Energy* **2007**, *32*, 4071–4080. [CrossRef]
13. Saravanan, N.; Nagarajan, G. Performance and emission studies on port injection of hydrogen with varied flow rates with Diesel as an ignition source. *Appl. Energy* **2010**, *87*, 2218–2229. [CrossRef]
14. Srinivasan, C.; Subramanian, R. Investigation of using hydrogen as an internal combustion engine fuel. *Middle East J. Sci. Res.* **2015**, *23*, 785–790.
15. Khandal, S.; Banapurmath, N.; Gaitonde, V. Effect of hydrogen fuel flow rate, fuel injection timing and exhaust gas re-circulation on the performance of dual fuel engine powered with renewable fuels. *Renew. Energy* **2018**, *126*, 79–94. [CrossRef]
16. Khandal, S.; Banapurmath, N.; Gaitonde, V. Effect of exhaust gas recirculation, fuel injection pressure and injection timing on the performance of common rail direct injection engine powered with honge biodiesel (BHO). *Energy* **2017**, *139*, 828–841. [CrossRef]
17. Duda, K.; Wierzbicki, S.; Smieja, M.; Mikulski, M. Comparison of performance and emissions of a CRDI diesel engine fuelled with biodiesel of different origin. *Fuel* **2018**, *212*, 202–222. [CrossRef]
18. Roy, S.; Ghosh, A.; Das, A.K.; Banerjee, R. A comparative study of GEP and an ANN strategy to model engine performance and emission characteristics of a CRDI assisted single cylinder diesel engine under CNG dual-fuel operation. *J. Nat. Gas Sci. Eng.* **2014**, *21*, 814–828. [CrossRef]
19. Kim, H.; Choi, B. The effect of biodiesel and bioethanol blended diesel fuel on nanoparticles and exhaust emissions from CRDI diesel engine. *Renew. Energy* **2010**, *35*, 157–163. [CrossRef]
20. Ashok, B.; Nanthagopal, K.; Saravanan, B.; Somasundaram, P.; Jegadheesan, C.; Chaturvedi, B.; Sharma, S.; Patni, G. A novel study on the effect lemon peel oil as a fuel in CRDI engine at various injection strategies. *Energy Convers. Manag.* **2018**, *172*, 517–528. [CrossRef]
21. Hohenberg, G.F. *Advanced Approaches for Heat Transfer Calculations*; SAE Technical Paper; SAE International: Warrendale, PA, USA, 1979; pp. 2788–2806. Available online: http://www.jstor.org/stable/44699090 (accessed on 7 July 2021).

22. Hayes, T.K.; Savage, L.D.; Sorenson, S.C. *Cylinder Pressure Data Acquisition and Heat Release Analysis on a Personal Computer*; SAE Technical Paper; SAE International: Warrendale, PA, USA, 1986.
23. Manjunath, N.; Rajashekhar, C.; Khan, T.Y.; Badruddin, I.A.; Kamangar, S.; Khandal, S. Augmented Turbulence for Progressive and Efficient Combustion in Biodiesel–Diesel Engine. *Arab. J. Sci. Eng.* **2019**, *44*, 7957–7966. [CrossRef]
24. Lee, C.S.; Park, S.W. An experimental and numerical study on fuel atomization characteristics of high-pressure diesel injection sprays. *Fuel* **2002**, *81*, 2417–2423. [CrossRef]
25. Leung, D.Y.C.; Luo, Y.; Chan, T.L. Optimization of Exhaust Emissions of a Diesel Engine Fuelled with Biodiesel. *Energy Fuels* **2006**, *20*, 1015–1023. [CrossRef]